Anisotropy in large-eddy simulations determined from SO(3) symmetry group

T. Hofbauer[†], J.M.L.M. Palma[†], L. Biferale[‡], and S.M.A. Gama[§]

† CEsA, Faculdade de Engenharia, Universidade do Porto, 4200-465 Porto, Portugal
‡ Dipartimento di Fisica, Università "Tor Vergata," and INFN, 00133 Roma, Italy
§ Departamento de Matemática Aplicada, and CMUP, Universidade do Porto, 4169-007 Porto, Portugal

Abstract. The issue of small-scale anisotropy in the context of eddy-viscosity-type subgrid-scale models is discussed in the present work. Recent developments in turbulence research suggest that anisotropy from large spatial scales are felt far into the inertial subrange of turbulence. This is of particular importance for subgrid-scale models of large-eddy simulations. To address this issue, we present solutions of the random-phase Kolmogorov flow at moderate Reynolds numbers using direct numerical simulations and large-eddy simulations with four subgrid-scale models: the Smagorinsky, the dynamic, the dynamic Clark, and the tensor-diffusivity models. The degree of anisotropy at different scales is analysed by decomposing the structure function into their irreducible representation of the **SO**(3) symmetry group. The results suggest that the dynamic model and the dynamic Clark model reproduce the statistical behaviour reasonably well, even in the anisotropic sectors at small length scales.

1. Introduction

Even though the Navier-Stokes equations can be solved numerically, its huge number of degrees of freedom for fully developed turbulent flows renders the solution exceedingly expensive at increasing Reynolds numbers. Despite the continuous growth of computer performance, the computation of all relevant time and length scales by means of direct numerical simulation (DNS) of most turbulent flows of practical interest will not be feasible in the near future. In large-eddy simulations (LES), the large, energy-containing scales are directly computed and the effect of the subgrid (also subfilter or unresolved) scales onto the resolved scales has to be modelled. The LES philosophy is based on Kolmogorov's theoretical predictions [1] which state that, in the limit of high Reynolds numbers, statistical quantities in the inertial subrange of turbulence

† Corresponding author. E-mail address: hofbauer@fe.up.pt

are universal, largely independent of both the forcing and dissipative mechanism. A byproduct of this is the restoration of isotropy towards smaller scales [2]. However, recent experimental and numerical results are not consistent with such local isotropy and show that anisotropies can persist far into the inertial subrange of turbulence [3–9], raising the question about the validity of Kolmogorov's *return-to-isotropy* hypothesis. The common understanding nowadays is that anisotropies are generally sub-leading with respect to the isotropic fluctuations. Still, due to the presence of intermittency also in the anisotropic correlation functions, anisotropies are found to decay much slower than what is predicted on the basis of dimensional analysis [10, 11], leading to the *apparently* puzzling result that, for high Reynolds numbers, some purely anisotropic observables vanish while others do not [5, 12]. The anomalous persistency of anisotropic contributions may have an even stronger signal in all LESs where the subgrid-scale is set, by the underlying assumption, in the inertial range. Therefore, in many common LES applications, large scale anisotropies may not have decayed enough to be negligible at the cut-off scale. However, since the eddy-viscosity concept, as basis of many SGS models, is intrinsically isotropic, one could argue that anisotropic contributions must vanish at the filter scales. Thus, the question arises, whether SGS models are capable of reproducing a proper level of anisotropy at the small scales.

A first attempt in this direction to answer these questions was made in [13], by communicating the results of an *a priori* test of the tensor-diffusivity model and investigated the scaling behaviour of both the isotropic and the anisotropic contributions in a random-phase Kolmogorov flow. As an outcome of the study, the tensor-diffusivity model, which was first proposed by Leonard [14], turned out to produce proper statistical behaviour for the isotropic contribution, but to fail to be fully accurate for the anisotropic counterparts.

In the present work, we will extend the scope by *a posteriori* testing of a variety of subgrid-scale (SGS) models, namely the classical Smagorinsky model (SMA), the dynamic Lagrangian model (DLM), the dynamic Clark model (DCM) and the tensor-diffusivity model (TDM); see [15] and [16] for reviews on subgrid-scale models. Herein, we test the degree of anisotropy by analysing velocity structure functions, which are then decomposed into its isotropic and anisotropic contributions by means of the **SO**(3) decomposition [17] (see [18] for a recent review). Additionally, we determine the actual scaling exponents, which we compare with the outcomes of other studies. The present work is organised as follows. In section 2, we briefly recapitulate the fundamentals of the structure functions and its scaling behaviour in the classical formulation with the decomposition and irreducible presentation of the **SO**(3) symmetry group. The governing equation and the general solution methodologies of the random-phase Kolmogorov flow are described together with a brief overview over the SGS models. The results are presented and discussed in section 3. Concluding remarks are given in section 4. **A more in-depth introduction of anisotropic turbulence requested by the referee.**   include

2. Background & Methodology

2.1. Anisotropic scaling behaviour

The phenomenological theory of isotropic and homogeneous turbulence of Kolmogorov assumes that, in the limit of high Reynolds numbers, the statistical quantities solely depend on the mean energy dissipation rate ϵ and the length scale $r = \|\mathbf{r}\|$ being within the inertial subrange of turbulence. The longitudinal pth-order structure function $S^{(p)}(r)$ exhibits a power-law behaviour in the inertial range:

$$S^{(p)}(r) \equiv \langle ([\mathbf{u}(\mathbf{x}+\mathbf{r},\, t) - \mathbf{u}(\mathbf{x},\, t)] \cdot \hat{\mathbf{r}})^p \rangle \propto (\epsilon\, r)^{\zeta(p)}, \tag{1}$$

where angle brackets denote averaging over space $(\mathbf{x})$ and time (t), $\mathbf{u}$ and $\zeta(p)$ are the fluid velocity and the scaling exponent, respectively. A growing body of evidence however suggests that, in the presence of anisotropic contents, it is not actually the structure function itself, but rather its decomposition into isotropic and anisotropic contributions that exhibits a true power-law behaviour. The technique used to untangle the isotropic and the –different– anisotropic contributions is based on the irreducible representations of the $\mathbf{SO}(3)$ symmetry group [17]. We must now allow a dependency on vector $\mathbf{r}$ for the structure function (1), which becomes a set of scalar functions of the three dimensional separation vector: $S^{(p)}(\mathbf{r})$. By projecting the pth-order structure function onto the different sectors of the irreducible representations of the $\mathbf{SO}(3)$ symmetry group, we decompose it into its isotropic and anisotropic contributions:

$$S^{(p)}(\mathbf{r}) = \sum_{j=0}^{\infty} \sum_{m=-j}^{j} S_{j,m}^{(p)}(r)\, Y_{j,m}(\hat{\mathbf{r}}), \text{ with } \hat{\mathbf{r}} = \mathbf{r}/\|\mathbf{r}\|, \tag{2}$$

where j and m are the eigenvalues of the rotational operator in three dimensions (the total angular momentum and its projection on one axis in the usual *quantum mechanical jargon*), and $Y_{j,m}(\hat{\mathbf{r}})$ are the spherical harmonics. The physics are now hidden in the coefficients of the decomposition. The isotropic fluctuations are captured by the $j = 0$ sector, $S_{0,0}^{(p)}(r)$, while more and more anisotropic contributions are described by the $S_{j,m}^{(p)}(r)$ at increasing values for j. Today, the existence of the scaling behaviour of the form

$$S_{j,m}^{(p)}(r) \propto a_{j,m}^{(p)} r^{\zeta_j(p)},$$

is generally accepted, where the scaling $r^{\zeta_j(p)}$ is supposed to be universal, while the prefactors $a_{j,m}^{(p)}$ depend on the large-scale physics of the flow [19]. Because the m eigenvalue depends on the chosen orientation of the z-axis, one does not expect a dependency of the scaling exponents on its value, see below. Moreover, a hierarchical organisation among exponents is observed: $\zeta_j(p) < \zeta_{j'}(p)$ with $j < j'$, supporting the idea that anisotropies are sub-leading with respect to the isotropic sector $j = 0$, c.f. [5, 8, 9, 20]. **Further details on the SO(3) methodology is found in the new Appendix.**

2.2. Governing equations of the random-phase Kolmogorov flow

We consider the motion of an incompressible Newtonian fluid $\partial u_i / \partial x_i = 0$ of unit density obeying the forced Navier-Stokes equations,

$$\frac{\partial u_i}{\partial t} + \frac{\partial (u_i \, u_k)}{\partial x_k} = -\frac{1}{\rho} \frac{\partial p}{\partial x_i} + \frac{\partial \tau_{ik}}{\partial x_k} + f \, \delta_{i3}, \tag{3}$$

in a cubic, tri-periodic domain with a side $L = 2\pi$, where $\mathbf{u} = (u_1, \, u_2, \, u_3)$, p and f denote the fluid velocity, pressure and external body force, respectively. Here and hereafter, the summation convention is used for repeated subscripts. In case of DNS, $\tau_{ik} = 2 \, \nu \, \mathcal{S}_{ik}$, where ν is the kinematic viscosity and $\mathcal{S}_{ik}$ is the strain-rate tensor.

Spatio-temporal homogeneity is achieved by the phase of the forcing which is random in space and δ-correlated in time, whereby $f = c \sin(\kappa x_1 + \phi(t))$, with $\phi(t)$ being a random variable uniformly distributed in $[0; 2\pi[$. Here, c and κ are a constant factor and the wavelength of the forcing, respectively. This is the so-called random-phase Kolmogorov flow [8]. The DNS uses a spatial resolution of 128^3 grid points corresponding to $R_\lambda \approx 50$. Let us stress here that our aim is twofold. First, we want to probe how much LES using different SGS models are able to reproduce the large-scales anisotropic contents of the Random Kolmogorov Flow. In order to do that, we fixed in all numerical simulations, for both DNS and LES, the same forcing mechanism, f, which gives the same energy input, ϵ, and the same large-scale geometry. Second, we want to probe how much different SGS model are able to increase the scaling range of anisotropic fluctuations by reducing the dissipative effects at the end of the inertial range. In order to achieve this second goal, we decided to run the DNS and the LES at two different resolutions, 128^3 and 64^3, resepctively, assessing the performance of different LES models depending on their ability to extend the scaling range beyond the interval possesed by the DNS. IN other words, our best LES model is the one that achieves, with respect to DNS, the longest inertial range with the smallest resolution. The code is based on a finite-volume approach, standard second-order central finite differences for spatial derivatives, a fractional-step algorithm, a Runge-Kutta (4/3) scheme for time derivatives and a collocated grid. For a detailed description and validation of the code, see [21].

2.3. Subgrid-scale modelling

In LES, equation (3) is filtered which leads to an additional term for the subgrid-scale stresses $(-\partial \tau_{ik}^{\mathrm{SGS}} / \partial x_k)$, where, dependent on the SGS model that is used, different formulations for τ_{ik}^{SGS} are used. In this work, implicit filtering is assumed. The cell-averaged values from the finite-volume approach are considered as filtered quantities, where the filter width corresponds to the grid spacing Δ. For the classical Smagorinsky model (SMA), the deviatoric part of this residual subgrid-scale stress is

$$\tau_{ik}^{\mathrm{SMA}} = -2 \left(C_S \, \widetilde{\Delta} \right)^2 |\widetilde{\mathcal{S}}| \, \widetilde{\mathcal{S}}_{ik} = -2 \, \nu_t \, \widetilde{\mathcal{S}}_{ik} \,, \tag{4}$$

where $|\widetilde{\mathcal{S}}| = (\widetilde{\mathcal{S}}_{ik}\widetilde{\mathcal{S}}_{ik})^{1/2}$, C_S is the Smagorinsky constant, and $\widetilde{\Delta}$ is the characteristic filter width (quantities marked with a tilde are resolved). In the dynamic Lagrangian model (DLM), $(C_S\widetilde{\Delta})^2$ in (4) is replaced by $C\widetilde{\Delta}^2$, where C is a function that depends on space and time and is determined on the basis of the resolved field. In this approach, the Lagrangian localization for the averaging procedure is used [22]. The formulation of the tensor-diffusivity model (TDM) is obtained by the truncated Taylor series expansion of the velocity, which is $\tau_{ik}^{\text{TDM}} = \widetilde{\Delta}^2(\partial\widetilde{u}_i/\partial x_l)(\partial\widetilde{u}_k/\partial x_l)$. The dynamic Clark model (DCM) is a mixed model, which is composed of a tensor-diffusivity model for the Leonard and cross terms plus a dynamic model. Its formulation reads

$$\tau_{ik}^{\text{DCM}} = \widetilde{\Delta}^2\frac{\partial\widetilde{u}_i}{\partial x_l}\frac{\partial\widetilde{u}_k}{\partial x_l} - 2C\,\widetilde{\Delta}^2\,|\widetilde{\mathcal{S}}|\,\widetilde{\mathcal{S}}_{ik}. \tag{5}$$

3. Results and discussion

3.1. Scaling behaviour of the decomposed structure function

In order to assess the ability of the different LES models to reproduce the typical anisotropic properties of the random-phase Kolmogorov flow, we concentrate in this paper on the **SO**(3) decomposition of the second-order longitudinal structure function:

$$S^{(2)}(\mathbf{r}) = \langle|\mathbf{u}(\mathbf{x}+\mathbf{r},\,t) - \mathbf{u}(\mathbf{x},\,t)\cdot\hat{\mathbf{r}}|^2\rangle = \sum_{j=0}^{\infty}\sum_{m=-j}^{j} S_{j,\,m}^{(2)}(r)\,Y_{j,\,m}(\hat{\mathbf{r}}), \tag{6}$$

averaged over both space ($\mathbf{x}$) and time (t). We averaged along a time span of the order of 40 eddy turnover times, based on the large scale dynamics. We find good convergence of the statistics for the isotropic sector $j = 0$ and the anisotropic components up to $j = 6$. For anisotropic contributions of higher j, both the amount of spatial/temporal samples as well as the insufficient angular resolution prevent from getting more reliable results. A general trend towards unfavourable signal-to-noise ratios can be observed for increasing total angular momenta j, which can be attributed to the higher geometrical complexity of their corresponding spherical harmonics $Y_{j,\,m}$. As a consequence, we restrict our investigation to a set of sectors that offer an adequate quality and favourable scaling properties for the DNS data.

At large spatial scales, the isotropic sector $S_{0,\,0}^{(2)}(r)$, as shown in figure 1, reveals a good scaling power-law behaviour with normalized r. At small scales, $r/\Delta_{LES} < 4$, the decomposed structure functions differ for mainly two reasons. Firstly, the DNS results show two different regimes: at large scales, the flow statistics indicate inertial range, i.e. the scaling exponent matches the value measured at high Reynolds numbers $\zeta(2) \sim 0.7$, while the small scales are influenced by the dissipation range and, as a result, a steeper slope is found. While the scaling properties for the dynamic model and the dynamic Clark model are practically unchanged towards smaller scales, the results for the Smagorinsky model show a scaling behaviour similar to the DNS. Since the classical Smagorinsky model is known to be more dissipative, this result is not surprising. However, the tensor-diffusivity model yields a more gentle slope at small
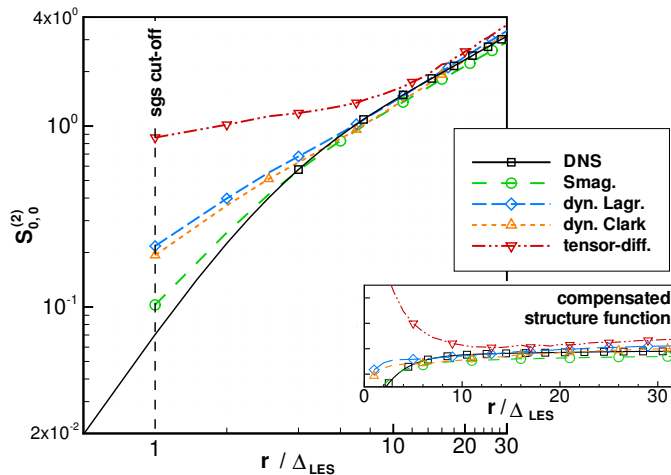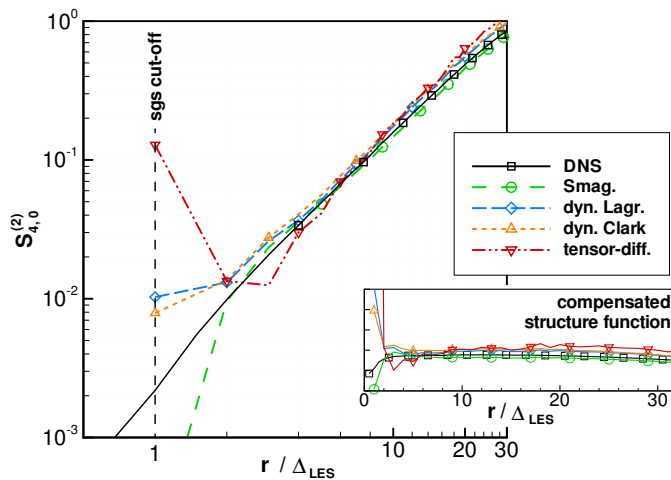
Figure 1. Isotropic component of the second-order velocity structure function $S_{0,0}^{(2)}(r)$ as a function of r for various LES models. Inset: Compensated plot with the power law behaviour of high Reynolds number, isotropic turbulence, $S_{0,0}^{(2)}(r)/r^{0.70}$ versus r.

scales over a range of one decade. This behaviour is due to the eddy-dissipation rate, which is positive on the average, but too low to be realistic. The failure of the tensor-diffusivity model even in the isotropic sector contradicts the results of the *a priori* tests carried out in [13]. Even though the deficiency has been pointed out many times, it seems important to us to stress again the inapplicability of the tensor-diffusivity model alone, without any additional model term that addresses the issue of the energy dissipation. Of course, any dynamical instability induced by the model can be detected only by means of *a posteriori* tests. This is probably the reason why the *a priori* investigation made in [13] was not able to detect such problems.

Let us now address the anisotropic contributions. We show in figure 2 an overall picture of all –measurable– isotropic and anisotropic sectors for the dynamic Lagrangian model, as an example of the general behaviour. As one can see, the isotropic sector is the leading one, being more intense at large scale and being the one with a slower decay toward small scales. Yet, the anisotropic sectors are not vanishing, supporting the statement that, for SGS models, anisotropies are important. For example, one may notice that anisotropies are still of the order of 10% at the subgrid cut-off. As a general rule, we observe that by increasing the level of anisotropy, the signal becomes less intense at large scales. Previous DNS data found the $j = 2$ sector affected by strong viscous effects [8]. We also find similar results in some of the LES models (see for example the bump in the $j = 2, m = 2$ curve in figure 2). Moreover, the $j = 2$ sector has a large-scale intensity which is always comparable with –or smaller than– the $j = 4$ sector. We therefore decide to concentrate on the scaling properties of the $j = 4$ and $j = 6$ anisotropic sectors, only. Note that, for odd values for j, the anisotropic contributions vanish either because of the parity of the structure function or due to the incompressibility constraint (see [18] for a detailed discussion of that issue). Good
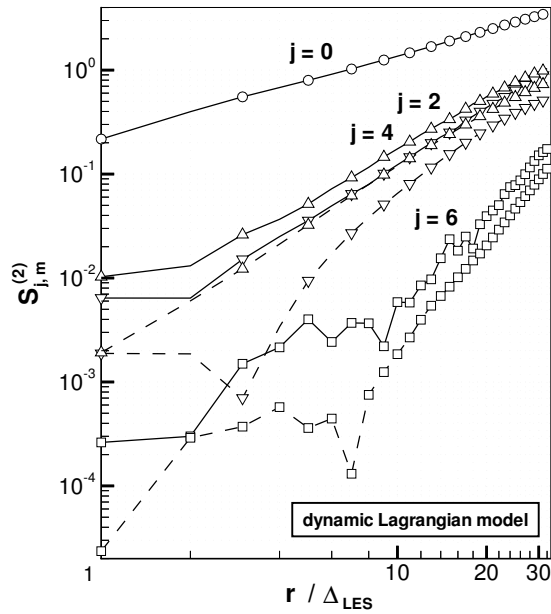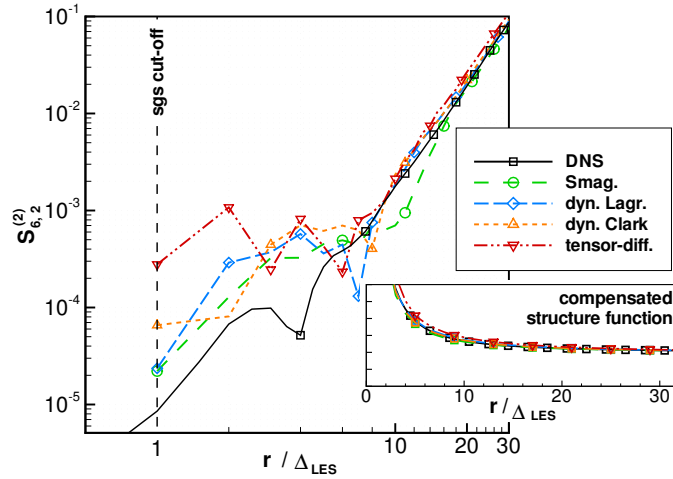
Figure 2. **SO**(3) decomposed structure function for the dynamic Lagrangian model (DLM); sectors $j = 0$ ($\bigcirc$), $j = 2$ ($\bigtriangledown$), $j = 4$ ($\triangle$), and $j = 6$ ($\square$); solid and dashed lines denote $m = 0$ and $m = 2$, respectively.

Figure 3. Decomposed structure function $S_{4,0}^{(2)}(r)$ versus r. Inset: compensate plots with th power law measured in DNS at higher resolution [8], $S_{4,0}^{(2)}(r)/r^{1.65}$.
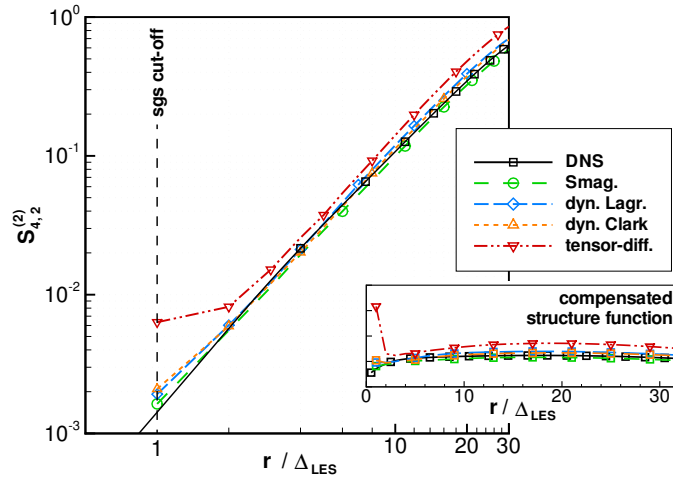
Figure 4. Anisotropic component $S_{4,2}^{(2)}(r)$ of the decomposed structure function vs. r. Inset: compensate plots with second power law measured in DNS at higher resolution [8], $S_{4,2}^{(2)}(r)/r^{1.65}$.

Figure 5. Decomposed second-order velocity structure function $S_{6,2}^{(2)}(r)$ as a function of r for various LES models. Inset: Compensated plot with the power law behaviour of high Reynolds number, isotropic turbulence, $S_{6,2}^{(2)}(r)/r^{3.2}$ versus r.

agreement between DNS and LESs is achieved for $S_{4,0}^{(2)}$ and $S_{4,2}^{(2)}(r)$ as it is shown in figures 3 and 4. All SGS models are able to reproduce the main feature of the anisotropic correlation function with the only exception of the TDM that is also here less accurate at scales of the order of the subgrid cut-off. Let us notice that the LES models are indeed working well leading to a slight increasing in the scaling range. The same, but for the $j = 6$ sector, is shown in figure 5. As can be deduced from figure 5 and previous figures, the data becomes more erratic towards higher angular momenta, because of the lack of statistical significance of less and less intense components. In summary, the presented results show the inapplicability of the tensor-diffusivity model. SMA, DLM

and DCM, which are all –at least partly– based on the eddy-viscosity concept, produce reasonable results.

3.2. Scaling exponents

The results presented above suggest a proper scaling behaviour in the isotropic and anisotropic sectors for DNS, SMA, DLM, and DCM. To verify our assumption in a more quantitative way, we determine the local scaling exponents $\zeta_{j,m}(2, r) = \partial \log(S_{j,m}^{(2)})/\partial \log(r)$ which are displayed scale-by-scale versus the normalized spatial scale $r^* = r/\Delta_{LES}$ in figure 6. First, the LES results display the hierarchy $\zeta_j(2) < \zeta_{j'}(2)$ if $j < j'$, that is observed in the DNS results. Second, we also find quite good robustness of $\zeta_{j,m}(2)$ for different eigenvalues m at a given j. This confirms that the scaling properties are independent of choice of the axis orientation.

In the isotropic sector ($j = 0$, $m = 0$), the scaling exponent is found to be close to constant over a wide range of scales r^*. The value of $\zeta_{j,m}(2, r)$ is in reasonable agreement with the numerical and experimental estimates of 0.7, confirming that LES models do not disfigure the intermittency measured in high Reynolds number flows. As has been already pointed out above, the values for DNS and SMA increase for $r^* \to 1$ due to the relatively high kinematic viscosity and eddy viscosity, respectively. The theoretical expectation $\zeta_{j=0}(2)|_{diss} = 2$ for the dissipation scales is not met, which indicates that only the transition to the dissipation range, rather than the dissipation range itself, is resolved in the DNS. What is remarkable is that both DLM and DCM yield scaling exponents in the isotropic sector that are close to constant over the entire range of r^*, which pinpoints the well-desired dilatation of the inertial range towards smaller scales, though the value is slightly more fluctuating when compared to DNS and SMA. Even stronger fluctuations, as well as scaling exponents well below the expectations, are found for the TDM, which again underlines its inapplicability in simulating turbulent flows. For the TDM in particular, and to a lesser degree for SMA, DLM and DCM, a general trend towards higher fluctuations of the scaling exponent is also observed in the anisotropic sector, while the mean value agrees reasonably well with the DNS result. As can be deduced also from sectors $(4, 0)$ and $(4, 2)$, figures 6b and 6c, the scaling exponents are slightly increasing for $r^* \to 1$ which, we argue, can be attributed to the unavoidable distortion of the grid structure. The comparison with higher resolution results in [8], estimating $\zeta_{j=4}(2) = 1.65 \pm 0.1$, is satisfactory. For sector $(6, 2)$, the numerical error in the determination of $\zeta_6(2)$ inherently increases, which arises from the increasing geometrical complexity of the basis functions and, as a result, to the lowered accuracy in determining the scaling exponent (curves are clipped for the sake of clarity, figure 6d). Although the amplitude of the fluctuations increases towards small r^*, the mean value is in reasonable agreement with large r^* values and the value $\zeta_{j=6}(2) = 3.2 \pm 0.2$ [8].
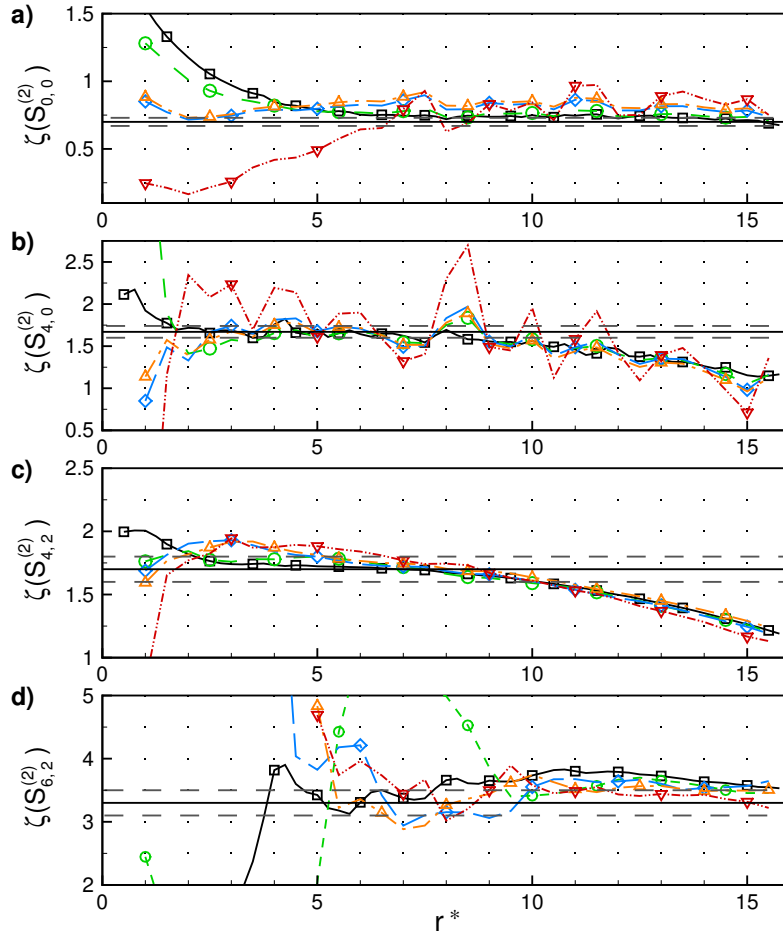
Figure 6. Scaling exponents $\zeta_{j,m}(2, r) = \partial \log(S_{j,m}^{(2)})/\partial \log(r)$ for the isotropic sector $(j, m) = (0, 0)$ and the anisotropic sectors $(4, 0)$, $(4, 2)$, and $(6, 2)$ for the DNS and different subgrid-scale models. Legend according to previous figures. The dashed straight lines describe the estimate of the scaling exponents from higher resoultion DNS, namely $\zeta_0(2) = 0.7 \pm 0.03$, $\zeta_4(2) = 1.67 \pm 0.07$ and $\zeta_4(2) = 1.7 \pm 0.1$ for $m = 0$ and $m = 2$, respectively, and $\zeta_6(2) = 3.3 \pm 0.2$.

4. Concluding remarks

Direct numerical simulations and large-eddy simulations of the random-phase Kolmogorov flow were performed in order to assess the accuracy of subgrid-scale models in representing small-scale anisotropies. The tensor-diffusivity model –without any additional term for an increased dissipation rate– is found to be inaccurate as a subgrid-scale model. Results from the Smagorinsky model, the dynamic model and the dynamic Clark model were in agreement with DNS data of higher resolution. The scaling behaviour, analysed by using the irreducible representations of the **SO**(3) symmetry group, shows that the latter SGS models can mimic the scaling at large scales. The isotropic and anisotropic scaling exponents $\zeta_j(2)$ agree reasonable well with previous studies conducted in this field. **(referee's 4th issue: universal range is small and** include

calculated values for the scaling exponents are therefore not very reliable.) Whereas LES and DNS results agree very well at the large scales, small deviations are found at small scales. The wavenumber range of these deviations are found to be dependent on the total angular momentum j and are up to $\mathcal{O}(10\Delta_{LES})$ for $j = 6$. This is unavoidable due to the weakness of the anisotropic signal at those scales. Additionally, distortion induced by the cubic grid may affect the **SO**(3) projections for small scale separation. The study presented here does not close the issue of whether LES models are able to faithfully reproduce the isotropic and anisotropic properties of turbulent flows. More refined tests on higher order statistical objects, such as structure functions of 4th and higher order, and on correlation functions involving observables at the grid scale would be a natural extension of this work.

Acknowledgments

Appendix

This appendix is solely intended to the readers who are not familiar with spherical harmonics and **SO**(3) machinery. In recent studies, e.g. [7], these mathematical tools revealed to be important for anisotropy analysis also in turbulence, after being used in other areas of knowlwedge, namely quantum mechanics. A fully, detailed and omnicomprehnsive description of the SO(3) decomposition of any tensorial quantities and of its application to Turbulence and other hydrodynamical systems can be found in [18].

The spherical harmonics, functions defined on the sphere, are special functions of mathematical physics and are directly connected to the classical orthogonal polynomials. A spherical harmonic is a single-valued, continuous, bounded, complex function of the angular coordinates θ and φ. Alternatively, the spherical harmonics are a complete basis for the irreducible representations of the infinite rotations group.

SO(3) is the group formed by the rotations (orientation-preserving rigid motions that fix the origin) in $\mathbb{R}^3$ and is isomorph to the set of all 3×3 matrices over $\mathbb{R}$ of determinant 1. **SO**(3) has precisely one irreducible representation in the space of 3d scalar functions, and no others. This representation may be realized in terms of $Y_{j,m}$, special functions known as *spherical harmonics*. The importance of **SO**(3) group theory in the study of anisotropy lies in the rotational invariance of Navier-Stokes equations

$$\text{Rotations } g_A^{\text{rot}} : \quad t, \mathbf{r}, \mathbf{u} \longrightarrow t, A\mathbf{r}, A\mathbf{u}, \quad A \in \mathbf{SO}(3),$$

in the unbounded domain limit. Anisotropy is studied by means of **SO**(3) decomposition

of the longitudinal structure function of order p

$$S_p(\mathbf{r}) = \langle \{ [\mathbf{u}\,(\mathbf{x} + \mathbf{r}) - \mathbf{u}\,(\mathbf{x})] \cdot \hat{\mathbf{r}} \}^p \rangle$$

where $\hat{\mathbf{r}} = \mathbf{r}/\|\mathbf{r}\|$ is the unity vector associated to $\hat{\mathbf{r}}$. It is a well known procedure to decompose scalar functions depending on $\hat{\mathbf{r}}$ into components of different irreducible representations using spherical harmonics (see Golubitsky *et al.* [26]). In particular, we can write

$$S_p(\mathbf{r}) = \sum_{j=0}^{+\infty} \sum_{m=-j}^{j} S_p^{jm}(\|\mathbf{r}\|)\, Y_{j,m}(\theta, \phi). \tag{7}$$

In this decomposition, the quantities $S_p^{j,m}(\|\mathbf{r}\|)$, that capture all the physical information contained in the longitudinal structure function, can be obtained thanks to (**??**). In fact, multiplying both sides of (7) by $Y_{\alpha\beta}^*(\theta, \phi)\, d(\cos\theta)$, integrating over $\cos\theta \in [-1, 1]$ and $\phi \in [0, 2\pi[$, and using (**??**), we get (rename α and β by j and m, respectively)

$$S_p^{j,m}(\|\mathbf{r}\|) = \int_0^{2\pi} d\phi \int_{-1}^{1} S_p(\mathbf{r})\, Y_{j,m}^*(\theta, \phi)\, d(\cos\theta).$$

In this paper the double integration above was performed by trapezoidal rule. Integration by Gaussian quadrature based on Legendre and Chebyshev polynomials were also carried out. In these three cases we were able to replicate the exact orthogonal condition (**??**). The scattering of data observed for high j components and small scales is due to the lack of precision in the numerical integration for such small signal amplitudes. It is a direct measurement of the signal-to-noise ratio in our numerical data and numerical post-processing of data.

References

[1] Kolmogorov A N 1941 Dissipation of energy in locally isotropic turbulence *Dokl. Akad. Nauk SSSR* **32** 16–18 (reprinted in *Proc. R. Soc. Lond.* A **434** 15–17 (1991))

[2] Frisch U 1995 *Turbulence: The Legacy of A. N. Kolmogorov* (Cambridge University Press, Cambridge)

[3] Shen X and Warhaft Z 2000 The anisotropy of the small scale structure in high Reynolds number ($R_\lambda \sim 1000$) turbulent shear flow *Phys. Fluids* **12**(11) 2976–89

[4] Shen X and Warhaft Z 2002 Longitudinal and transverse structure functions in sheared and unsheared wind-tunnel turbulence *Phys. Fluids* **14**(1) 370–81

[5] Shen X and Warhaft Z 2002 On the higher order mixed structure functions in laboratory shear flow *Phys. Fluids* **14**(7) 2432–38

[6] Arad I, Dhruva B, Kurien S, L'vov V S, Procaccia I and Sreenivasan K R 1998 Extraction of anisotropic contributions in turbulent flows *Phys. Rev. Lett.* **81**(24) 5330–3

[7] Arad I, Biferale L, Mazzitelli I, and Procaccia I 1999 Disentangling scaling properties in anisotropic and inhomogeneous turbulence *Phys. Rev. Lett.* **82** 5040-3

[8] Biferale L and Toschi F 2001 Anisotropic homogeneous turbulence: hierarchy and intermittency of scaling exponents in the anisotropic sectors *Phys. Rev. Lett.* **86**(21) 4831–34

[9] Kurien S, L'vov V, Procaccia I, and Sreenivasan K R 2000 Scaling structure of the velocity statistics in atmospheric boundary layers *Phys. Rev. E* **61** 407–21

[10] Lumley J L 1967 Similarity and the turbulence energy spectrum *Phys. Fluids* **10**, 855–58

[11] Biferale L, Daumont I, Lanotte A, and Toschi F 2002 Anomalous and Dimensional scaling in anisotropic turbulence *Phys. Rev. E* **66** 056306

[12] Biferale L and Vergassola M 2001 Isotropy vs anisotropy in small-scale turbulence *Phys. Fluids* **13**(8) 2139-41

[13] Biferale L, Daumont I, Lanotte A and Toschi F 2004 Theoretical and numerical study of highly anisotropic turbulent flows *Eur. J. Mech. B/Fluids* **23**(3) 401-14

[14] Leonard A 1974 Energy cascade in large-eddy simulations of turbulent flows *Adv. Geophys.* **18** 237–248

[15] Sagaut P 2003 *Large Eddy Simulation for Incompressible Flows – An Introduction* 2nd edn(Berlin:Springer)

[16] Meneveau C and Katz J 2000 Scale-Invariance and Turbulence Models for Large-Eddy Simulations *Annu Rev. Fluid Mech.* **32** 1–32

[17] Arad I, L'vov V S and Procaccia I 1999 Correlation functions in isotropic and anisotropic turbulence: The role of the symmetry group *Phys. Rev. E* **59**(6) 6753–65

[18] Biferale L and Procaccia I 2004 Anisotropy in turbulent flows and in turbulent transport *submitted to Phys. Rep.* (arXiv:nlin.CD/0404014)

[19] Biferale L, Calzavarini E, Toschi F, and Tripiccione R 2003 Universality of anisotropic fluctuations from numerical simulations of turbulent flows *Europhys. Lett.* **64** 461–7

[20] Kurien S and Sreenivasan K R 2000 Anisotropic scaling contributions to high-order structure functions in high-Reynolds-number turbulence *Phys. Rev. E* **62** 2206–12

[21] Lopes A S and Palma J M L M 2001 Numerical simulation of isotropic turbulence using a collocated approach and a non-orthogonal grid system *J. Comp. Phys.* **175** 713–38

[22] Armenio V and Piomelli U 2000 A Lagrangian mixed subgrid-scale model in generalized coordinates *Flow, Turbulence and Combustion* **65** 51–81

[23] Biferale L, Boffetta G, Celani A, Lanotte A, Toschi F and Vergassola M 2003 The decay of homogeneous anisotropic turbulence *Phys. Fluids* **15**(8), 2105–12

[24] Nikiforov A F and Uvarov V B 1988 Special functions of mathematical physics. Birkhäuser.

[25] Press H P, Teukolsky S A, Vetterling W T and Glannery B P 1992 Numerical Recipes in Fortran: the Art of Scientific Computing (2nd Edition). Cambridge University Press.

[26] Golubitsky M, Stewart I and Schaeffer D G 1988 Singularities and groups in bifurcation theory (Vol. II) Springer-Verlag